

# SIMULATION OF NONLINEAR DIFFUSION ON A SPHERE

Yuri N. Skiba

*Centre for Atmospheric Sciences (CCA), National Autonomous University of Mexico (UNAM)  
Av. Universidad 3000, C.P. 04510, Mexico City, Mexico*

Denis M. Filatov

*Centre for Computing Research (CIC), National Polytechnic Institute (IPN)  
Av. Juan de Dios Batiz s/n, C.P. 07738, Mexico City, Mexico*

**Keywords:** Simulation of environmental problems, Nonlinear diffusion, Split finite difference schemes.

**Abstract:** A new numerical technique for the simulation of nonlinear diffusion processes on a sphere is developed. The core of our approach is to split the original equation's operator, thus reducing the two-dimensional problem to two one-dimensional problems. Further, we apply two different coordinate grids to cover the entire sphere for solving the split 1D problems. This allows avoiding the question of imposing adequate boundary conditions near the poles, which is always a serious problem when modelling on a sphere. Yet, therefore we can employ finite difference schemes of any even approximation order in space. The developed approach is cheap to implement from the computational point of view. Numerical experiments prove the suggested technique, simulating several diffusion phenomena with high accuracy.

## 1 INTRODUCTION

A large number of important natural phenomena, e.g., heat transfer in ionised gases, unconfined groundwater flow and gas percolation through porous media, viscous liquid flows over smooth horizontal substrates — just to name a few — are described by nonlinear diffusion equations (Bear, 1988; Lacey et al., 1982; Peletier, 1981; Seshadri and Na, 1985; Wu et al., 2001). Many of them, in particular those arising in environmental problems, are normally studied on a sphere, which implies considering a nonlinear diffusion equation in the spherical geometry in the form

$$\frac{\partial T}{\partial t} = AT + f, \quad (1)$$

where

$$AT \equiv \frac{1}{R \cos \varphi} \left[ \frac{\partial}{\partial \lambda} \left( \frac{D}{R \cos \varphi} \frac{\partial T}{\partial \lambda} \right) + \frac{\partial}{\partial \varphi} \left( \frac{D \cos \varphi}{R} \frac{\partial T}{\partial \varphi} \right) \right], \quad (2)$$

subject to an appropriate initial condition. Here  $A$  is the diffusion operator,  $T = T(\lambda, \varphi, t) \geq 0$  is the function to be sought (depending on the application, it can be the density of a substance, the temperature, etc.),  $D = \mu T^\alpha$  is the diffusion coefficient,  $\mu =$

$\mu(\lambda, \varphi, t) > 0$  is the normalisation factor,  $f = f(\lambda, \varphi, t)$  is the source function,  $R$  is the radius of the sphere  $S$ ,  $\lambda \in [0, 2\pi)$  is the longitude,  $\varphi \in (-\pi/2, +\pi/2)$  is the latitude. Since the term  $\cos \varphi$  vanishes at  $\varphi = \pm\pi/2$ , the sphere's poles are singularities, so the solution has always to be treated carefully there. The parameter  $\alpha$  is normally a positive integer that determines the degree of nonlinearity of the diffusion process; the case  $\alpha = 0$  corresponds to the linear diffusion.

Usually, real problems do not allow finding the exact analytical solution, and therefore numerical methods have to be used.

In this work we suggest an efficient numerical method for the simulation of nonlinear diffusion processes on a sphere using a second- and a fourth-order finite difference schemes. The keypoint of our approach is to split the original diffusion operator by coordinates (Marchuk, 1982). This allows to consider the resulting one-dimensional problems in  $\lambda$  and in  $\varphi$  on two different coordinate grids, periodic each in its own direction. Therefore, we avoid the problem of imposing suitable boundary conditions at the pole singularities, which is always a challenge when studying a partial differential equation on a sphere. Otherwise, an additional procedure would be required to enclose Eq. (1) on the boundary, which may either complicate

the solution from the computational standpoint or disturb it by introducing nonphysical modes.

The rest of the paper is organised as follows: in Section 2 we present a mathematical background of the suggested numerical method, and in Section 3 we prove it on several numerical tests aimed to simulate nonlinear diffusion phenomena. Conclusions are given in Section 4.

## 2 MATHEMATICAL BACKGROUND

Introduce the following notation  $\tau = t_{n+1} - t_n$ ,  $\Delta\lambda = \lambda_{k+1} - \lambda_k$ ,  $\Delta\varphi = \varphi_{l+1} - \varphi_l$ , and split Eq. (1) in every sufficiently small time interval  $(t_n, t_{n+1})$  by coordinates (Marchuk, 1982)

$$\frac{\partial T}{\partial t} = \frac{1}{R \cos \varphi} \frac{\partial}{\partial \lambda} \left( \frac{D}{R \cos \varphi} \frac{\partial T}{\partial \lambda} \right) + \frac{f}{2}, \quad (3)$$

$$\frac{\partial T}{\partial t} = \frac{1}{R \cos \varphi} \frac{\partial}{\partial \varphi} \left( \frac{D \cos \varphi}{R} \frac{\partial T}{\partial \varphi} \right) + \frac{f}{2}. \quad (4)$$

To treat the pole singularities, we exclude the poles by defining a shifted in  $\Delta\varphi/2$  grid on  $S$  in the form

$$S_{\Delta\lambda, \Delta\varphi}^{(1)} = \left\{ (\lambda_k, \varphi_l) : \lambda_k \in \left[ \frac{\Delta\lambda}{2}, 2\pi + \frac{\Delta\lambda}{2} \right), \right. \\ \left. \varphi_l \in \left[ -\frac{\pi}{2} + \frac{\Delta\varphi}{2}, \frac{\pi}{2} - \frac{\Delta\varphi}{2} \right] \right\}. \quad (5)$$

This grid will be employed for solving Eq. (3): to do this, we merely use periodic boundary conditions in  $\lambda$ . For solving Eq. (4), we take another coordinate grid, with the same nodes as (5), —

$$S_{\Delta\lambda, \Delta\varphi}^{(2)} = \left\{ (\lambda_k, \varphi_l) : \lambda_k \in \left[ \frac{\Delta\lambda}{2}, \pi - \frac{\Delta\lambda}{2} \right], \right. \\ \left. \varphi_l \in \left[ \frac{\Delta\varphi}{2}, 2\pi + \frac{\Delta\varphi}{2} \right] \right\}. \quad (6)$$

The benefit of employing grid (6) is that we can use periodic boundary conditions in  $\varphi$  instead of imposing adequate boundary conditions if we used (5). Hence, due to the grid swap we use periodic boundary conditions while computing in *both* directions, although the sphere is *not* a doubly periodic domain, as well.

Discretising the temporal derivatives in (3) and (4), we have

$$\frac{\partial T}{\partial t} \Big|_{t=t_n} \approx \frac{T_k^{n+1/2} - T_k^n}{\tau} \quad \text{for all } l\text{'s} \quad (7)$$

and

$$\frac{\partial T}{\partial t} \Big|_{t=t_{n+1/2}} \approx \frac{T_l^{n+1} - T_l^{n+1/2}}{\tau} \quad \text{for all } k\text{'s}, \quad (8)$$

respectively. Note that both approximations, (7) and (8), are computed in the interval  $(t_n, t_{n+1})$  (of the length  $\tau$ ), *not* in  $(t_n, t_{n+1/2})$  and  $(t_{n+1/2}, t_{n+1})$  (of the length  $\tau/2$ ).

Because of the periodicity of the solution in both directions due to the grid swap, we are free in choosing an approximation stencil for the discretisation of the spatial derivatives in space. For example, taking

$$\frac{\partial}{\partial \lambda} \left( D \frac{\partial T}{\partial \lambda} \right) \Big|_{\lambda=\lambda_k} \approx \frac{1}{\Delta\lambda} \left( D_{k+1/2} \frac{T_{k+1} - T_k}{\Delta\lambda} - D_{k-1/2} \frac{T_k - T_{k-1}}{\Delta\lambda} \right), \quad (9)$$

$$\frac{\partial}{\partial \varphi} \left( D \cos \varphi \frac{\partial T}{\partial \varphi} \right) \Big|_{\varphi=\varphi_l} \approx \frac{1}{\Delta\varphi} \left( D_{l+1/2} \cos \varphi_{l+1/2} \frac{T_{l+1} - T_l}{\Delta\varphi} - D_{l-1/2} \cos \varphi_{l-1/2} \frac{T_l - T_{l-1}}{\Delta\varphi} \right), \quad (10)$$

we obtain the simplest second-order schemes. (The terms at the semi-integer nodes are computed in a standard way as half sums thereof taken from the two nearest integer nodes.) For increasing the schemes' accuracy, we first differentiate by parts as follows

$$\frac{\partial}{\partial \lambda} \left( D \frac{\partial T}{\partial \lambda} \right) = \frac{\partial D}{\partial \lambda} \frac{\partial T}{\partial \lambda} + D \frac{\partial^2 T}{\partial \lambda^2}, \quad (11)$$

$$\frac{1}{\cos \varphi} \frac{\partial}{\partial \varphi} \left( D \cos \varphi \frac{\partial T}{\partial \varphi} \right) = \left( \frac{\partial D}{\partial \varphi} - D \tan \varphi \right) \frac{\partial T}{\partial \varphi} + D \frac{\partial^2 T}{\partial \varphi^2} \quad (12)$$

and then discretise the right-hand sides of (11)-(12). The differentiation by parts allows reducing the size of the resulting schemes' stencils. So, for the fourth-order approximation we find the schemes to be only five-pointed

$$\frac{\partial D}{\partial \lambda} \frac{\partial T}{\partial \lambda} + D \frac{\partial^2 T}{\partial \lambda^2} \Big|_{\lambda=\lambda_k} \approx \frac{-D_{k+2} + 8D_{k+1} - 8D_{k-1} + D_{k-2}}{12\Delta\lambda} * \\ \frac{-T_{k+2} + 8T_{k+1} - 8T_{k-1} + T_{k-2}}{12\Delta\lambda} + \\ D_k \frac{-T_{k+2} + 16T_{k+1} - 30T_k + 16T_{k-1} - T_{k-2}}{12\Delta\lambda^2}, \quad (13)$$

$$\left. \left( \frac{\partial D}{\partial \varphi} - D \tan \varphi \right) \frac{\partial T}{\partial \varphi} + D \frac{\partial^2 T}{\partial \varphi^2} \right|_{\varphi=\varphi_l} \approx \left( \frac{-D_{l+2} + 8D_{l+1} - 8D_{l-1} + D_{l-2}}{12\Delta\varphi} - D_l \tan \varphi_l \right) \frac{-T_{l+2} + 8T_{l+1} - 8T_{l-1} + T_{l-2}}{12\Delta\varphi} + D_l \frac{-T_{l+2} + 16T_{l+1} - 30T_l + 16T_{l-1} - T_{l-2}}{12\Delta\varphi^2}, \quad (14)$$

whereas nine-pointed schemes would appear if we approximated the spatial derivatives in Eqs. (3)-(4) directly, without the prior differentiation by parts (Gibou and Fedkiw, 2005).

The temporal discretisation of the spatial terms can be taken, say, as an implicit approximation, i.e.  $T_{kl} := T_{kl}^{n+j/2}$ , where  $j = 1$  while computing in  $\lambda$  and  $j = 2$  while computing in  $\varphi$ . As for the nonlinear diffusion term itself, we linearise the schemes taking for  $T_{kl}^\alpha$  the solution from the previous time interval  $(t_{n-1}, t_n)$ , i.e.  $T_{kl}^\alpha := T_{kl}^{n\alpha}$ .

In (Skiba and Filatov, 2011), for the linear diffusion equation, it was shown that the constructed second- and fourth-order finite difference operators are negative definite and the corresponding schemes are dissipative, according to the properties of the original (differential) diffusion equation. Since the approximation  $T_{kl}^\alpha = T_{kl}^{n\alpha}$  provides linearised finite difference schemes, the established results are also true for the schemes developed in the current paper. Besides, due to the splitting and the grid swap technique the constructed schemes eventually appear as systems of linear algebraic equations with band matrices. Therefore, the simulation of nonlinear diffusion phenomena can be carried out by direct and inexpensive numerical methods — say, for the second-order schemes with three-diagonal matrices the fast Thomas algorithm can be used (Press et al., 2007). And last but not least, the periodicity of the boundary conditions in both directions also guarantees the solution to the split problem to converge to the solution to the original (unsplit) problem while  $\tau \rightarrow 0$  (Marchuk, 1982).

### 3 NUMERICAL SIMULATION

We shall test the developed method, simulating a few interesting diffusion problems. Specifically, we shall consider linear diffusion of a spot located at a pole, as well as prove the approach both on linear and nonlinear problems comparing the numerical solutions vs. the analytics. The analytical solutions are chosen in an arbitrary manner, since our goal is mainly to test the accuracy of the developed

numerical method and to show that it can be used for performing adequate simulation at all.

**Problem 1.** Under  $\alpha = 0$  and  $\mu = const$  we choose the function

$$T(\lambda, \varphi, t) = ((\lambda - \pi) \sin \lambda)^2 \sin^2 \varphi \cos^2 t + 1 \quad (15)$$

as the exact (analytical) solution. This function satisfies Eq. (1) if

$$f(\lambda, \varphi, t) = -\frac{2\mu \cos^2 t}{R^2 \cos \varphi} (f_1 + f_2) - f_3, \quad (16)$$

where

$$\begin{aligned} f_1(\lambda, \varphi) &= \cos^{-1} \varphi \sin^2 \varphi * \\ &(\sin^2 \lambda + 2(\lambda - \pi) \sin 2\lambda + (\lambda - \pi)^2 \cos 2\lambda), \\ f_2(\lambda, \varphi) &= ((\lambda - \pi) \sin \lambda)^2 \cos \varphi * \\ &(\cos 2\varphi - \sin^2 \varphi), \\ f_3(\lambda, \varphi, t) &= ((\lambda - \pi) \sin \lambda)^2 \sin^2 \varphi \sin 2t. \end{aligned} \quad (17)$$

The initial condition  $T(\lambda, \varphi, 0)$  on the grid  $S_{\Delta\lambda, \Delta\varphi}^{(1)}$  is shown in Fig. 1.

Comparing the numerical solutions with the analytics, we compute the relative errors

$$\delta(t) \equiv \frac{\|\Delta T\|_{L_2}}{\|T^{exact}\|_{L_2}} = \frac{\sqrt{\sum_{kl} (T_{kl}^{num} - T_{kl}^{exact})^2 \Delta S}}{\sqrt{\sum_{kl} (T_{kl}^{exact})^2 \Delta S}}. \quad (18)$$

Graphs of the  $\delta$ 's in time for the second- and the fourth-order schemes on the grid  $6^\circ \times 6^\circ$  are shown in Fig. 2. In Fig. 3 we also plot the  $L_2$ -norm of the exact solution given by (15). As one can see, the maximum error does not exceed 1% for the second-order scheme, and it is smaller than 0.5% for the fourth-order one. The errors also demonstrate periodical growth and decay in time, similarly to the

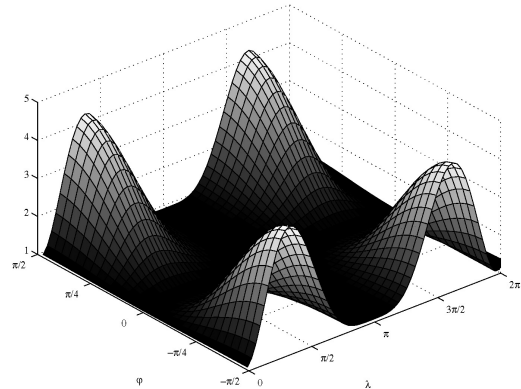


Figure 1: Problem 1: Initial condition  $T(\lambda, \varphi, 0)$ .

behaviour of the  $L_2$ -norm of the analytical solution.

**Problem 2.** Let the initial condition be a spot located at the north pole. We take  $\alpha = 0$  and introduce a non-constant asymmetric diffusion coefficient of the form (Fig. 4)

$$\mu(\lambda, \varphi) = \sin \frac{\lambda}{2} \sin^2 \varphi. \quad (19)$$

The asymmetry introduced by  $\sin \frac{\lambda}{2}$  has the aim to make sure the grid swap (5)-(6) does not disturb the solution by introducing any artificial errors near the poles. If it does, unphysical effects in the solution will be observed.

The numerical solution computed on the grid  $6^\circ \times 6^\circ$  shows that the spot is spreading in accordance with the diffusion coefficient's form: the diffusion process is mainly observed where  $\mu$  achieves its maximum ( $\lambda = \pi$ ), whereas less diffusion happens where  $\mu$  is most negligible ( $\lambda \approx 0$ ) (Figs. 5). No other effects are observed (cf. Fig. 4).

**Problem 3.** To apply the developed schemes to nonlinear diffusion problem, we take  $\alpha = 2$  and  $\mu = 1 \cdot 10^{-7}$ , while for the exact solution we choose

$$T(\lambda, \varphi, t) = 20 \sin \xi \cos \varphi \cos^2 t + 300, \quad (20)$$

$$\xi \equiv \omega \lambda + \vartheta \cos \kappa \varphi \sin t.$$

Then, substituting (20) into (1), for the sources we find

$$f(\lambda, \varphi, t) = -\frac{20\mu T^{\alpha-1} \cos^2 t}{R^2 \cos \varphi} (f_1 + f_2 + f_3) + f_4, \quad (21)$$

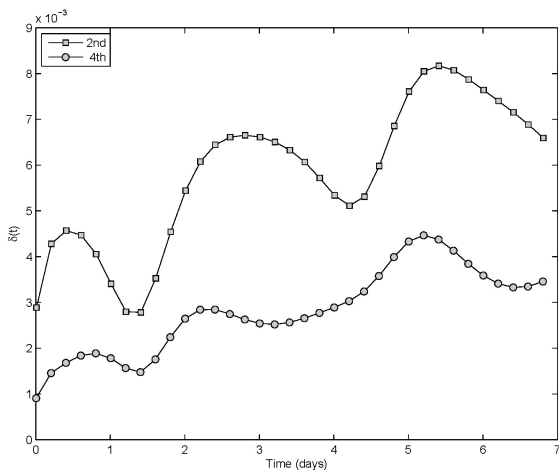


Figure 2: Problem 1: Relative errors  $\delta(t)$  for the second- and the fourth-order schemes.

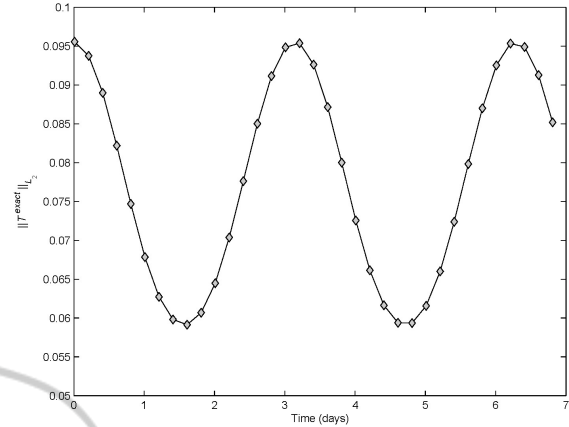


Figure 3: Problem 1:  $L_2$ -norm of the analytical solution (15).

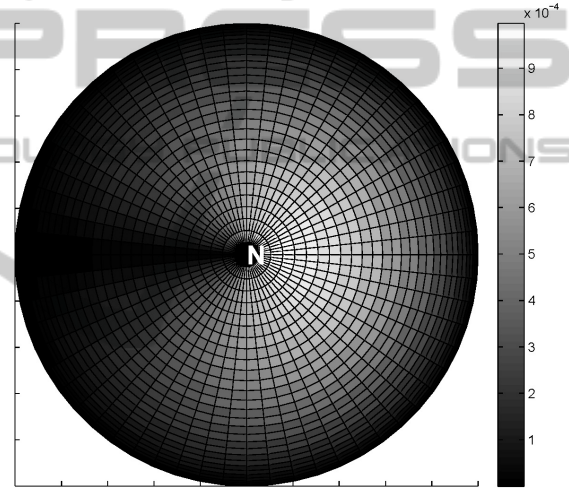


Figure 4: Problem 2: Form of the diffusion coefficient (19), pole view.

where

$$f_1(\lambda, \varphi, t) = 20\alpha \cos \varphi \cos^2 t (\omega^2 \cos^2 \xi + \sin \varphi * \sin \xi (\kappa \vartheta \sin t \cos \xi \sin \kappa \varphi \cos \varphi + \sin \xi \sin \varphi)),$$

$$f_2(\lambda, \varphi, t) = T \sin \xi (\sin^2 \varphi - \cos^2 \varphi - \omega^2),$$

$$f_3(\lambda, \varphi, t) = \kappa \vartheta \sin t \cos \varphi * [20\alpha \cos \xi \sin \kappa \varphi \cos \varphi \cos^2 t * (\kappa \vartheta \sin t \cos \xi \sin \kappa \varphi \cos \varphi + \sin \xi \sin \varphi) - T (\kappa \vartheta \sin t \sin \xi \sin^2 \kappa \varphi \cos \varphi + \cos \xi (\kappa \cos \kappa \varphi \cos \varphi - 3 \sin \kappa \varphi \sin \varphi))],$$

$$f_4(\lambda, \varphi, t) = 20 \cos \varphi (\vartheta \cos \kappa \varphi \cos \xi \cos^3 t - \sin \xi \sin 2t). \quad (22)$$

We assume  $\omega = 7$ ,  $\vartheta = 7\pi/2$ ,  $\kappa = 3$ .

In Fig. 6 we plot graphs of the relative errors  $\delta(t)$  in time for the second- and the fourth-order schemes,

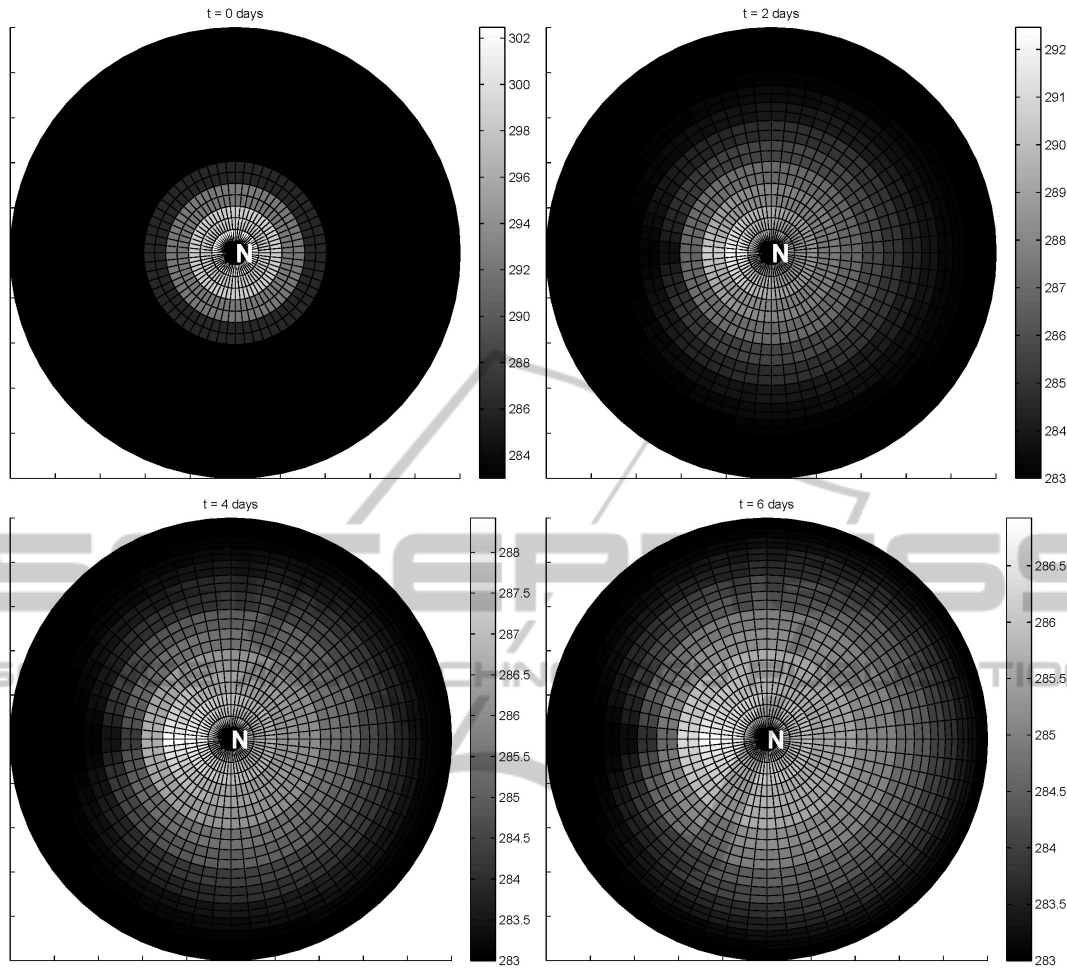


Figure 5: Problem 2: Diffusion of a (north-)pole-located spot at various time moments (4th-order scheme, pole view).

while in Fig. 7 we show the temporal behaviour of the  $L_2$ -norm of the exact solution (20).

One can observe that the fourth-order scheme yields better results than the second-order one ( $\max \delta(t)$  0.05 vs. 0.075). Yet, the relative errors demonstrate periodical behaviour, similar to the analytical solution, which indicates the operator splitting provides accurate approximations to the original unsplit differential problem. As for period doubling, this phenomenon is due to the structure of the solution (20).

As for the solution itself (Figs. 8), it is properly behaving according to the term  $\sin \xi$ . Specifically, as the time  $t$  grows, the sinusoid begins travelling to the west at low latitudes and to the east at high ones, since the phase shift  $\vartheta \cos \kappa \varphi \sin t$  is positive for  $\varphi \approx 0$  and negative for  $\varphi \approx \pm \frac{\pi}{2}$  at small times. When the time comes to  $t = \frac{\pi}{2}$ , the direction of rotation is changed to the opposite one, etc. This is exactly what one can

observe in Figs. 8 for a few time moments.

## 4 CONCLUSIONS

We have developed a new numerical technique for the simulation of nonlinear diffusion processes in the spherical geometry when the computational domain is the entire sphere. The core of the technique consists in performing splitting of the original operator by coordinates and subsequent grid swap. This approach allows constructing second- and fourth-order finite difference schemes efficiently implementable as systems of linear algebraic equations with band matrices. Numerical tests have proved the approach to provide highly accurate results and to be suitable for simulating both linear and nonlinear diffusion phenomena on a sphere.

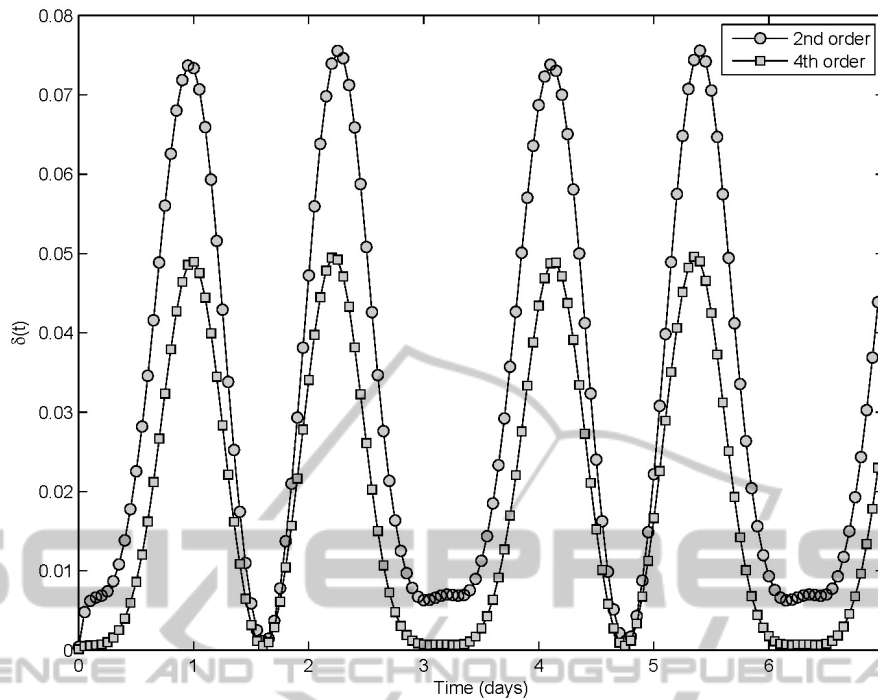


Figure 6: Problem 3: Relative errors  $\delta(t)$  for the second- and the fourth-order schemes.

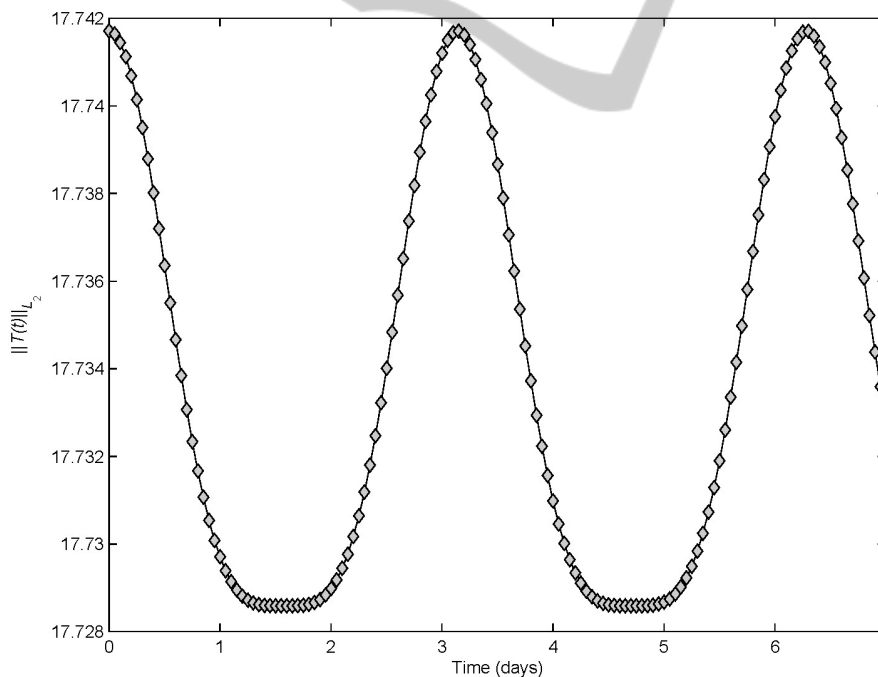


Figure 7: Problem 3:  $L_2$ -norm of the analytical solution (20).

## ACKNOWLEDGEMENTS

This research was partially supported by the grants No. 14539 and No. 26073 of the National System

of Researchers of Mexico (SNI), and is part of the projects PAPIIT-UNAM IN105608, FOSEMARNAT-CONACyT 2004-01-160, Mexico.

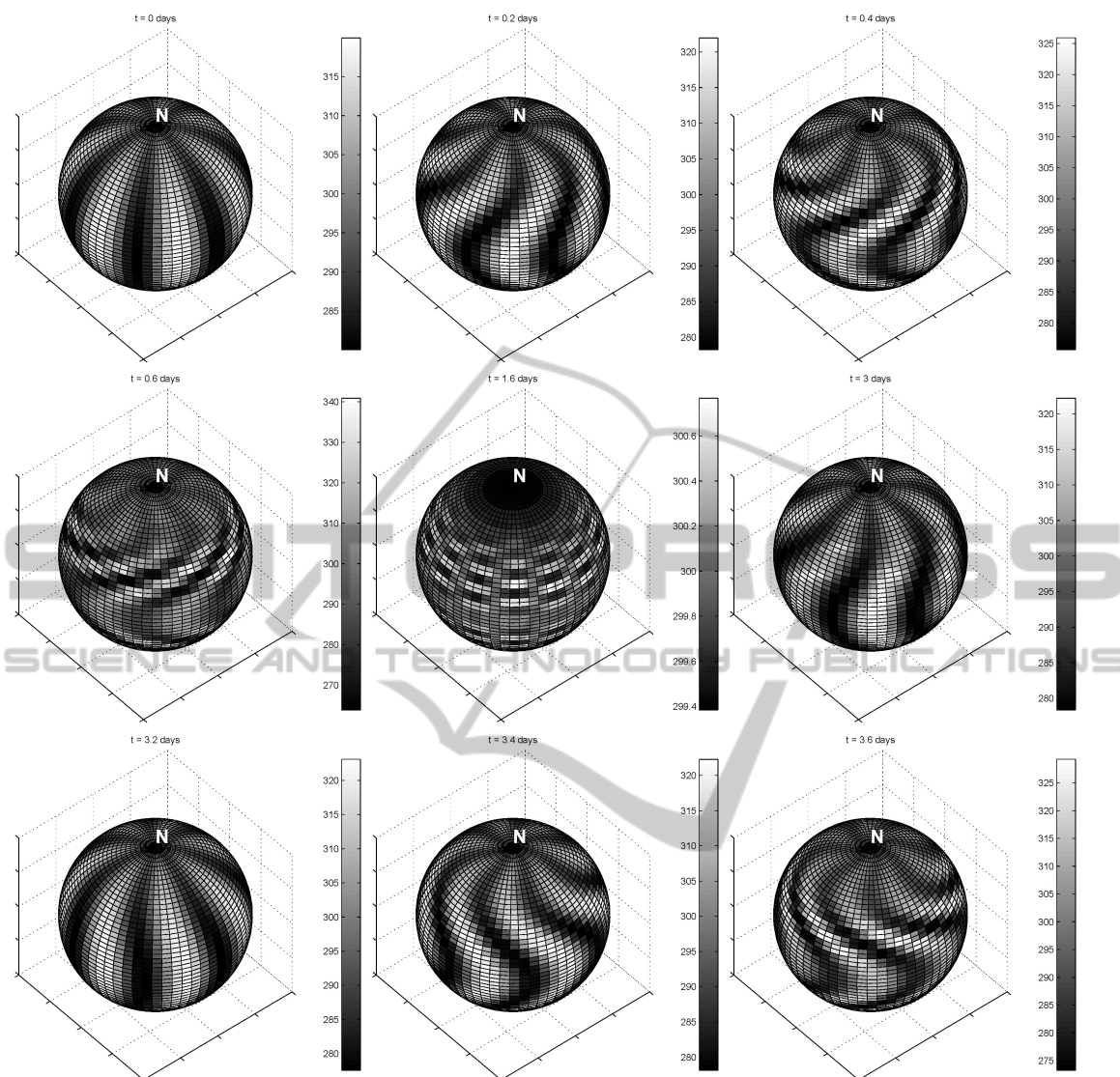


Figure 8: Problem 3: Numerical solution at several time moments (2nd-order scheme, grid  $6^\circ \times 6^\circ$ ).

## REFERENCES

- Bear, J. (1988). *Dynamics of Fluids in Porous Media*. Dover Publications, New York.
- Gibou, F. and Fedkiw, R. (2005). A fourth order accurate discretization for the laplace and heat equations on arbitrary domains, with applications to the stefan problem. *J. Comput. Phys.*, 202:577–601.
- Lacey, A. A., Ockendon, J. R., and Tayler, A. B. (1982). “waiting-time” solutions of a nonlinear diffusion equation. *SIAM J. Appl. Math.*, 42:1252–1264.
- Marchuk, G. I. (1982). *Methods of Computational Mathematics*. Springer-Verlag, Berlin.
- Peletier, L. A. (1981). The porous media equation. In Ammam, H. and Bazley, N., editors, *Applications of Non-linear Analysis in the Physical Sciences*, pages 229–241. Pitman, Boston.
- Press, W. H., Teukolsky, S. A., Vetterling, W. T., and Flannery, B. P. (2007). *Numerical Recipes: The Art of Scientific Computing*. Cambridge University Press, Cambridge.
- Seshadri, R. and Na, T. Y. (1985). *Group Invariance in Engineering Boundary Value Problems*. Springer-Verlag, New York.
- Skiba, Y. N. and Filatov, D. M. (2011). On an efficient splitting-based method for solving the diffusion equation on a sphere. *Numer. Meth. Part. Diff. Eq.*, 27:doi: 10.1002/num.20622.
- Wu, Z., Zhao, J., Yin, J., and Li, H. (2001). *Nonlinear Diffusion Equations*. World Scientific Publishing, Singapore.